Electronic Supplementary Material (ESI) for Nanoscale.


# Supporting Information

*Landon Oakes[1,2], Rachel Carter[2], and Cary L. Pint[1,2]*

1. Interdisciplinary Materials Science and Engineering, Vanderbilt University, Nashville, TN, 37212
2. Mechanical Engineering, Vanderbilt University, Nashville, TN, 37212

*Address correspondence to cary.l.pint@vanderbilt.edu

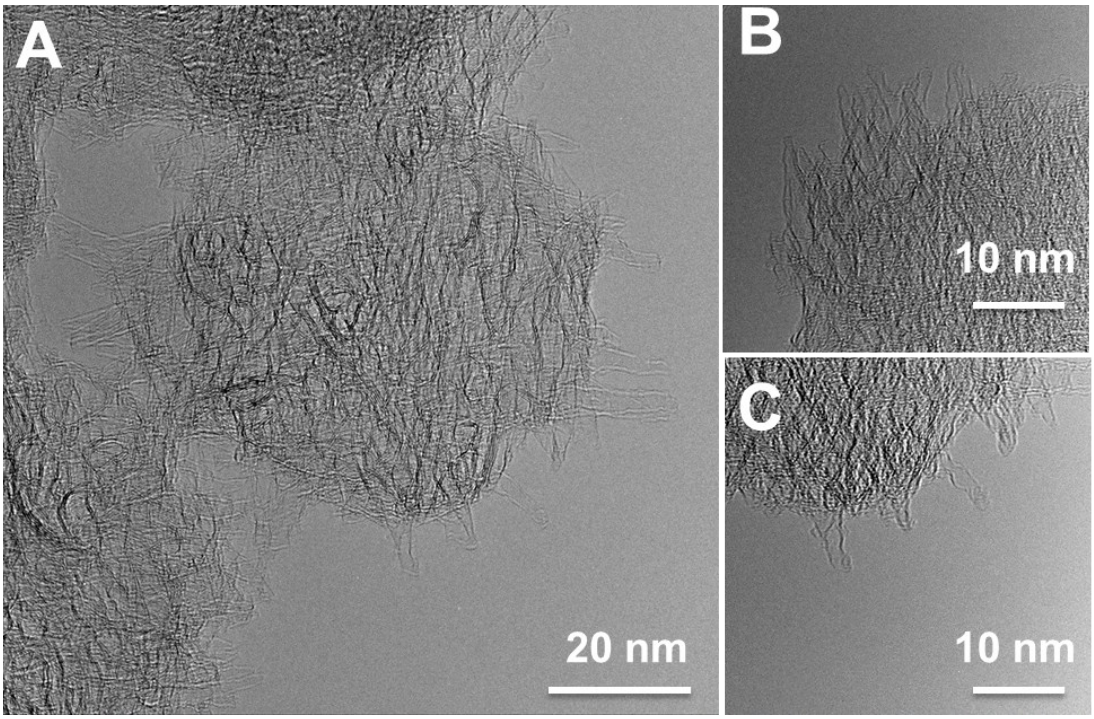


**Figure S1.** TEM analysis of the CNHs used in this study. (A) TEM of an individual CNH emphasizing the tortuous, defective nature of the carbon comprising the CNH. (B,C) Zoomed-in analysis of the edges of the CNH illustrating the conical carbon terminations characteristic of CNH materials.

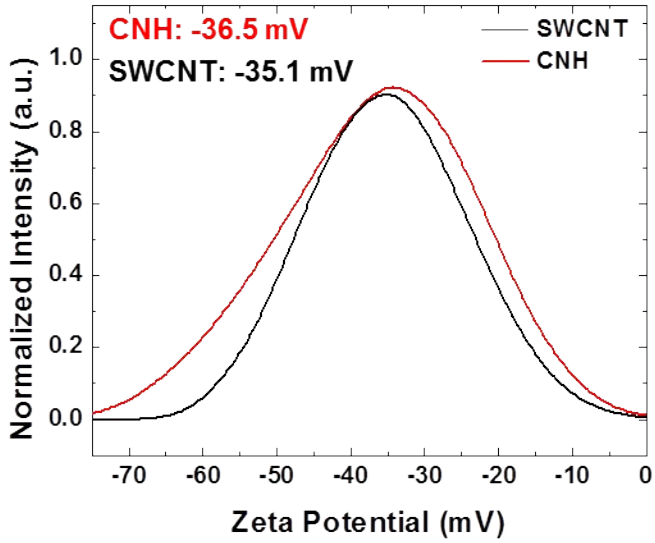


**Figure S1.** Zeta potential measurements of NMP solutions of the nanostructures used in this study. Measurements were performed on solutions with a concentration of 50 μg/ml.

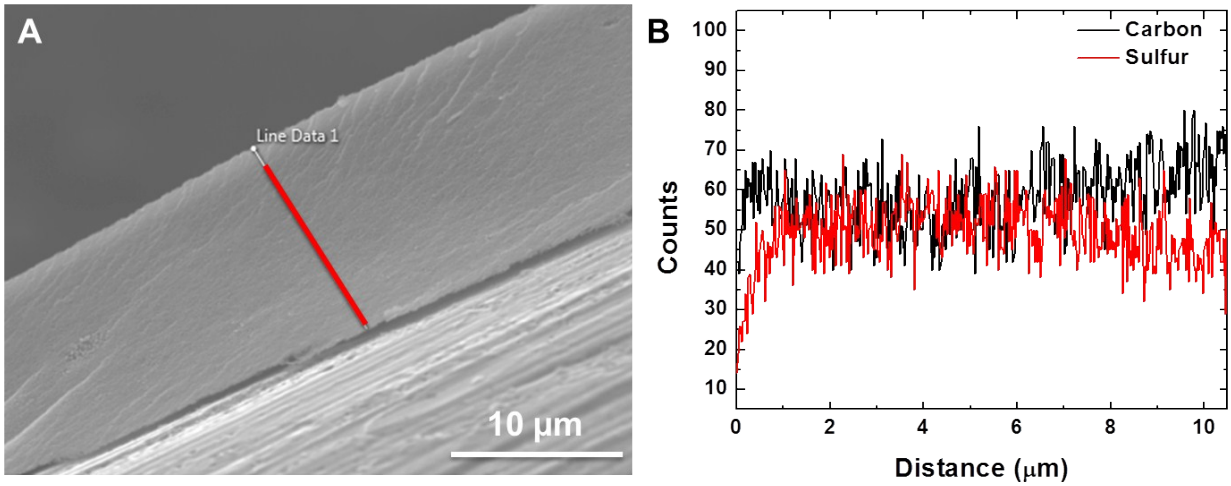


**Figure S2.** (A) SEM image of a 70% CNH cross-sectional sample infiltrated to 75 wt.% sulfur. The red line inset describes the location of the EDS elemental analysis performed to investigate the uniformity of the sulfur coating. (B) Corresponding EDS linescan emphasizing the uniformity of the sulfur content throughout the entirety of the carbon film.

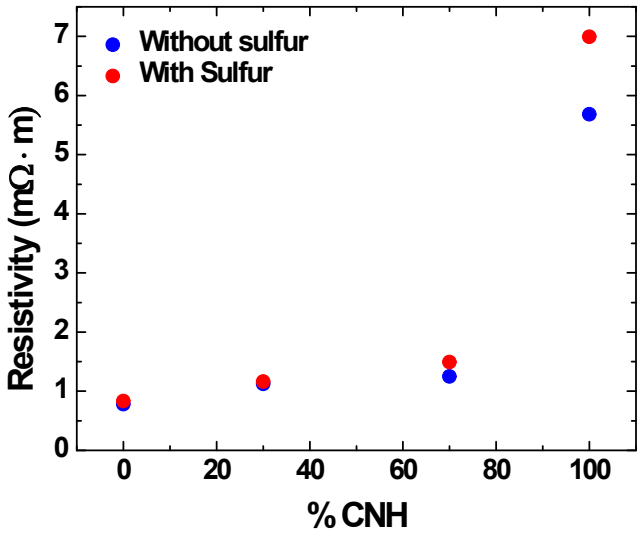


**Figure S3.** Resistivity measurements of the different hybrid materials before and after sulfur coating.

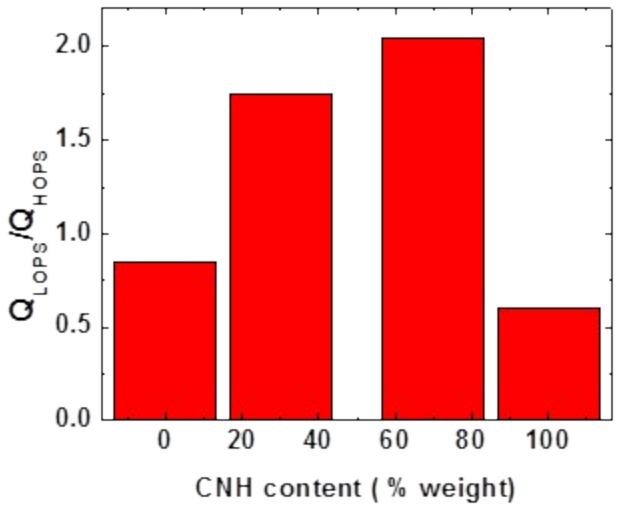


**Figure S4.** An analysis of the LOPS to HOPS for the rate study presented in Fig. 5A.

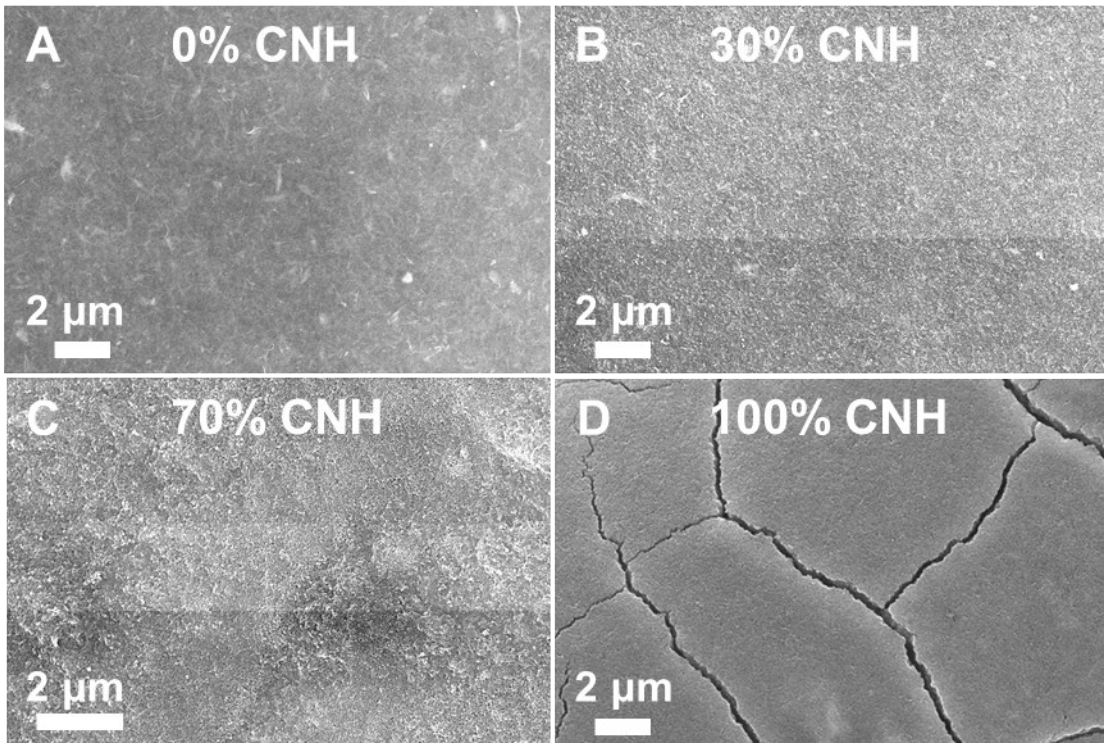


**Figure S5.** SEM characterization of the large-scale morphologies of the material systems used in this study. Insets indicate the amount of CNH loading present in each system. From these images, it is evident that the SWCNTs impart structural stability to the films and those lacking the presence of any SWCNTs have demonstrate cracking and delamination.

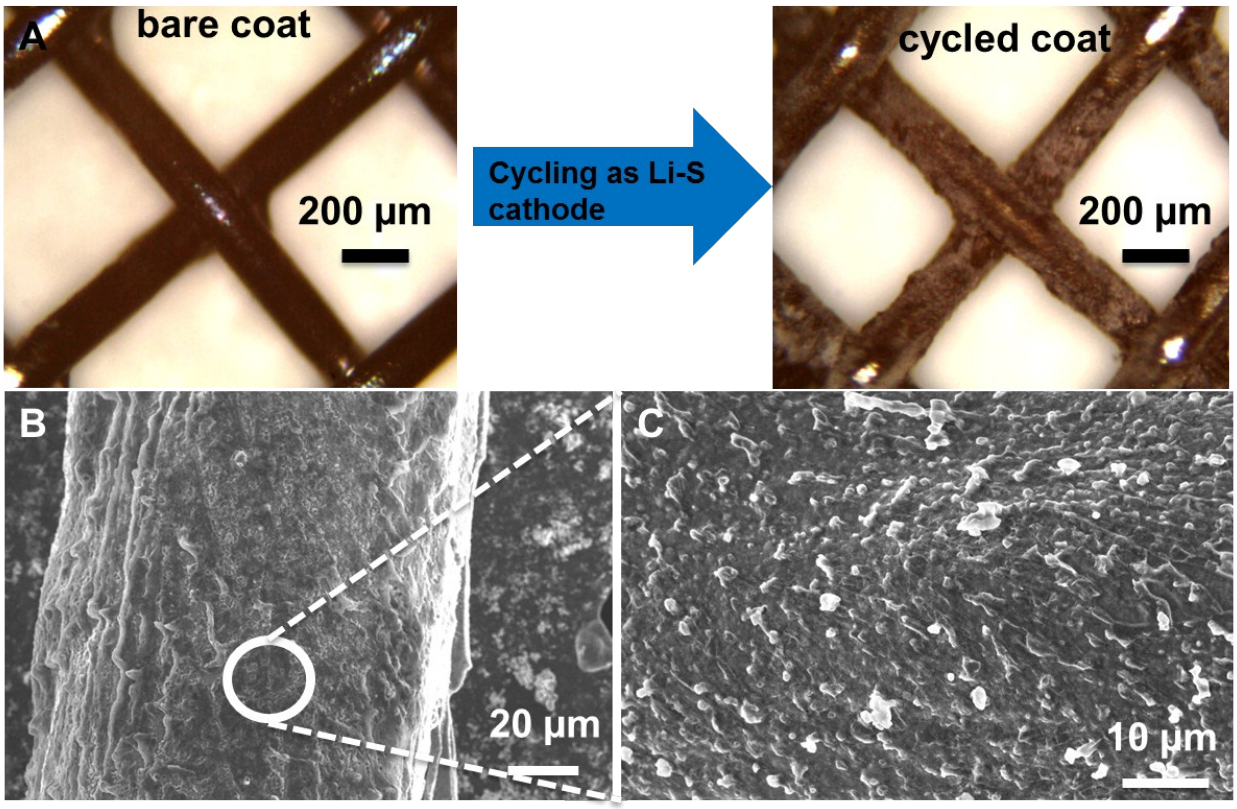


**Figure S6.** (A) Optical image of the coated mesh before and after cycling. The light colored residue on the cycled mesh electrode is due to dried electrolyte on the samples. (B) SEM characterization of the coated electrode after 10 charge-discharge cycles at a rate of 0.1 C emphasizing the stable adhesion of the carbon-sulfur composite on the mesh after cycling. (C) Higher magnification image of the sample in (B) demonstrating uniformity of the coating at small scales.

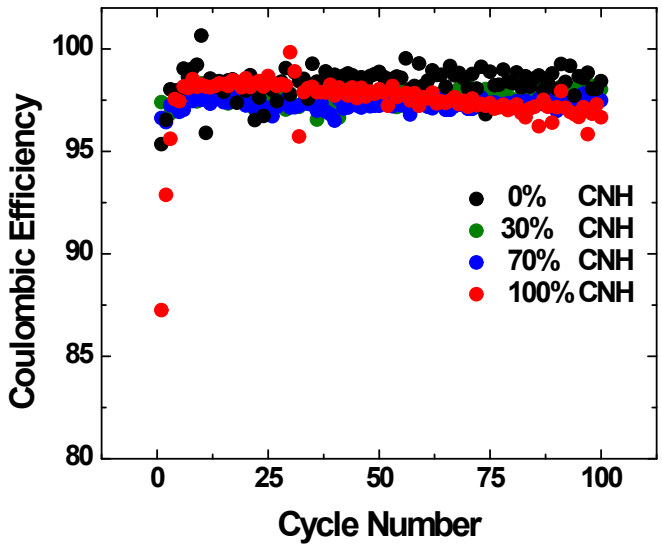


**Figure S7.** Coulombic efficiency for the devices cycled at 0.2 C.

| ref. | capacity (mAh/g) | loading (%) | additives (S:CB:binder) | utilization ( mAh/g ) |
|---|---|---|---|---|
| 1 | 1400 | 37 | binder-free | 518 |
| 2 | 1382 | 72 | 80:10:10 | 995.04 |
| 3 | 1368 | 52.5 | 70:10:20 | 718.2 |
| 4 | 1374 | 59 | 80:10:10 | 810.66 |
| 5 | 1219 | 53 | binder-free | 646.07 |
| 6 | 1633 | 68 | 80:10:10 | 1110.44 |
| 7 | 1120 | 56 | 75:10:15 | 627.2 |
| 8 | 1264 | 60 | binder-free | 758.4 |
| 9 | 1239 | 72 | 80:10:10 | 892.08 |
| 10 | 1070 | 56 | binder-free | 599.2 |
| 11 | 1400 | 35 | 70:20:10 | 490 |
| 12 | 1048 | 50 | binder-free | 524 |
| 13 | 1246 | 63.7 | 85:12:03 | 793.702 |
| 14 | 1346 | 62 | binder-free | 834.52 |
| 15 | 1340 | 62 | binder-free | 830.8 |
| 16 | 1021 | 57.12 | 80:10:10 | 583.1952 |
| 17 | 1260 | 58.4 | 80:15:10 | 735.84 |
| 18 | 911 | 53 | binder-free | 482.83 |
| 19 | 1317 | 48.3 | 70:20:10 | 636.111 |
| 20 | 1070 | 53.6 | 80:12:08 | 573.52 |
| 21 | 1310 | 63 | binder-free | 825.3 |
| 22 | 1620 | 65 | binder-free | 1053 |
| 23 | 800 | 52 | binder-free | 416 |
| 24 | 750 | 76.5 | 85:15:00 | 573.75 |
| 25 | 1010 | 62 | 90:10:00 | 626.2 |
| 26 | 1278 | 47.25 | 75:15:10 | 603.855 |
| 27 | 998 | 33.6 | 70:15:15 | 335.328 |

**Table S1**. Detailed description of the relevant parameters used to generate the plot in Figure 5. In order to calculate utilization, the sulfur loading was multiplied by the discharge capacity.

**REFERENCES**


1. Cui, Y., et al., *A binder-free sulfur/carbon composite electrode prepared by a sulfur sublimation method for Li-S batteries.* RSC Advances, 2016. **6**(58): p. 52642-52645.
2. Li, G., et al., *Three-dimensional porous carbon composites containing high sulfur nanoparticle content for high-performance lithium-sulfur batteries.* Nature communications, 2016. **7**.
3. Tao, X., et al., *Balancing surface adsorption and diffusion of lithium-polysulfides on nonconductive oxides for lithium-sulfur battery design.* Nature communications, 2016. **7**.
4. Yu, M., et al., *Atomic layer deposited TiO 2 on a nitrogen-doped graphene/sulfur electrode for high performance lithium–sulfur batteries.* Energy & Environmental Science, 2016. **9**(4): p. 1495-1503.
5. Li, R., et al., *Mildly reduced less defective graphene oxide/sulfur/carbon nanotube composite films for high-performance lithium–sulfur batteries.* Physical Chemistry Chemical Physics, 2016. **18**(16): p. 11104-11110.
6. Jin, F., et al., *Efficient Activation of High-Loading Sulfur by Small CNTs Confined Inside a Large CNT for High-Capacity and High-Rate Lithium–Sulfur Batteries.* Nano letters, 2015. **16**(1): p. 440-447.
7. Liang, X., et al., *A highly efficient polysulfide mediator for lithium–sulfur batteries.* Nature communications, 2015. **6**.
8. Sun, L., et al., *Sulfur Embedded in a Mesoporous Carbon Nanotube Network as a Binder-Free Electrode for High-Performance Lithium–Sulfur Batteries.* ACS nano, 2015. **10**(1): p. 1300-1308.
9. Du, W.-C., et al., *Wet Chemistry Synthesis of Multidimensional Nanocarbon–Sulfur Hybrid Materials with Ultrahigh Sulfur Loading for Lithium–Sulfur Batteries.* ACS applied materials & interfaces, 2015. **8**(6): p. 3584-3590.
10. Yuan, G., et al., *A novel three-dimensional sulfur/graphene/carbon nanotube composite prepared by a hydrothermal co-assembling route as binder-free cathode for lithium–sulfur batteries.* Journal of Nanoparticle Research, 2015. **17**(1): p. 1-11.
11. Kim, J.W., et al., *Improvement of Energy Capacity with Vitamin C Treated Dual-Layered Graphene–Sulfur Cathodes in Lithium–Sulfur Batteries.* ChemSusChem, 2015. **8**(17): p. 2883-2891.
12. Sun, L., et al., *Super-aligned carbon nanotube/graphene hybrid materials as a framework for sulfur cathodes in high performance lithium sulfur batteries.* Journal of Materials Chemistry A, 2015. **3**(10): p. 5305-5312.
13. Strubel, P., et al., *ZnO Hard Templating for Synthesis of Hierarchical Porous Carbons with Tailored Porosity and High Performance in Lithium-Sulfur Battery.* Advanced Functional Materials, 2015. **25**(2): p. 287-297.
14. Zhou, G., Y. Zhao, and A. Manthiram, *Dual-Confined Flexible Sulfur Cathodes Encapsulated in Nitrogen-Doped Double-Shelled Hollow Carbon Spheres and Wrapped with Graphene for Li–S Batteries.* Advanced Energy Materials, 2015. **5**(9).
15. Xi, K., et al., *Soluble polysulphide sorption using carbon nanotube forest for enhancing cycle performance in a lithium–sulphur battery.* Nano Energy, 2015. **12**: p. 538-546.
16. Qu, Y., et al., *Highly ordered nitrogen-rich mesoporous carbon derived from biomass waste for high-performance lithium–sulfur batteries.* Carbon, 2015. **84**: p. 399-408.
17. Xu, C., et al., *Sulfur/three-dimensional graphene composite for high performance lithium–sulfur batteries.* Journal of Power Sources, 2015. **275**: p. 22-25.
18. Chen, Y., et al., *Flexible Carbon Nanotube–Graphene/Sulfur Composite Film: Free-Standing Cathode for High-Performance Lithium/Sulfur Batteries.* The Journal of Physical Chemistry C, 2015. **119**(19): p. 10288-10294.

19. Guo, J., et al., *Microporous carbon nanosheets derived from corncobs for lithium–sulfur batteries.* Electrochimica Acta, 2015. **176**: p. 853-860.
20. Liu, S., et al., *A 3D nanostructure of graphene interconnected with hollow carbon spheres for high performance lithium–sulfur batteries.* Journal of Materials Chemistry A, 2015. **3**(21): p. 11395-11402.
21. Wang, C., et al., *Macroporous free-standing nano-sulfur/reduced graphene oxide paper as stable cathode for lithium-sulfur battery.* Nano Energy, 2015. **11**: p. 678-686.
22. Fu, K., et al., *Sulfur gradient-distributed CNF composite: a self-inhibiting cathode for binder-free lithium–sulfur batteries.* Chemical Communications, 2014. **50**(71): p. 10277-10280.
23. Xi, K., et al., *Binder free three-dimensional sulphur/few-layer graphene foam cathode with enhanced high-rate capability for rechargeable lithium sulphur batteries.* Nanoscale, 2014. **6**(11): p. 5746-5753.
24. Cheng, X.-B., et al., *Aligned carbon nanotube/sulfur composite cathodes with high sulfur content for lithium–sulfur batteries.* Nano Energy, 2014. **4**: p. 65-72.
25. Yang, X., et al., *Sulfur-infiltrated graphene-based layered porous carbon cathodes for high-performance lithium–sulfur batteries.* ACS nano, 2014. **8**(5): p. 5208-5215.
26. Zhao, C., et al., *Sulfur-infiltrated porous carbon microspheres with controllable multi-modal pore size distribution for high energy lithium–sulfur batteries.* Nanoscale, 2014. **6**(2): p. 882-888.
27. Jung, D.S., et al., *Hierarchical porous carbon by ultrasonic spray pyrolysis yields stable cycling in lithium–sulfur battery.* Nano letters, 2014. **14**(8): p. 4418-4425.